Coupled Systems Mechanics, *Vol. 14, No. 1 (2025) 43-55*
https://doi.org/10.12989/csm.2025.14.1.043

Design optimization of a coupling with bolted rim by way of MATLAB & ANSYS

Mubina Nancy[1a], S. Elizabeth Amudhini Stephen[∗1] and G. Hemalatha[2b]

[1]*Department of Mathematics, Karunya Institute of Technology and Sciences, Coimbatore, Tamil Nadu 641114, India*
[2]*Department of Civil Engineering, Karunya Institute of Technology and Sciences, Coimbatore, Tamil Nadu 641114, India*

(Received March 23, 2022, Revised February 14, 2025, Accepted February 21, 2025)

Abstract. In this work, the effectiveness of coupling with a bolted rim is assessed using newly developed optimization techniques. This paper examines and contrasts ten contemporary metaheuristic approaches for linking design optimization with fastened rims. Subjective and statistical evaluations are used to assess these algorithms' performance. Additionally, the problem's outcome is verified through the use of ANSYS simulation.

Keywords: ANSYS simulation; coupling with bolted rim; meta-heuristic; non-traditional optimization

1. Introduction

Giraud-Moreau and Lafon present the coupling with bolted rim problem. In mechanical transmission design, couplings are frequently used (Laurence *et al.* 2002). Couplings are built in a variety of constructive ways in applications, making a unified and commonly accepted classification challenging (Hammoudi *et al.* 2019). Light towers, air pumps, welding sets, and other gear with significant driving inertia have all used coupling in the past. The connection is made up of two cast iron hubs, a super- elastic rubber element, and locking hardware. In a stiff coupling, torque is supplied from one part of the coupling to the other by bolts, and shafts must be aligned in this configuration. Consider the simple mechanism shown in Fig. 1, which is made up of only a few basic connections and is designed to transmit torque between two coaxial shafts by adhesion (Aliriza *et al.* 2019).

2. Mathematical modelling (Lafon *et al.* 1994)

∗Corresponding author, Professor, E-mail: elizi.felix@gmail.com
[a]Ph.D.
[b]Professor

http://www.techno-press.org/?journal=csm&subpage=8 ISSN: 2234-2184 (Print), 2234-2192 (Online)

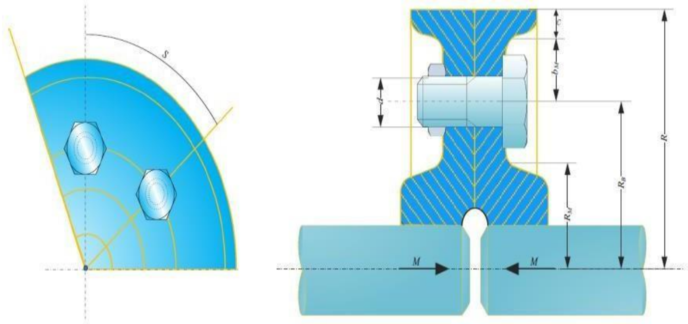

Fig. 1 Coupling bolted rim

Minimize: $f(x) = \beta_1\left(\frac{N'}{N_M}\right) + \beta_2\left(\frac{R_B+\phi_4(d)+c}{R_M}\right) + \beta_3\left(\frac{M}{M_T}\right)$

Subject to the constraints:

$$g_1(x) = \frac{\alpha M'}{N R_B K(d)} - 1 \le 0$$
$$g_2(x) = 1 - \frac{2\pi RB}{\phi_5(d)N} \le 0$$
$$g_3(x) = 1 - \frac{R_B}{\phi_4(d)N} + R_M$$
$$g_4(x) = N - N_{max} \le 0$$
$$g_5(x) = R - R_{max} \le 0$$
$$g_6(x) = N_m - N \le 0$$
$$g_7(x) = R_M - R_B \le 0$$
$$g_8(x) = M - M_{max} \le 0$$
$$g_9(x) = M_T - M \le 0$$
$$g_{10}(x) = d - 24 \le 0$$
$$g_{11}(x) = 6 - d \le 0$$
$$K(d') = \frac{0.9 f_m R_e \pi(\phi(d))^2}{4\sqrt{1+3((0.16\phi_3(d))\cdot f_1/\phi_1(d))^2}}$$

$\phi_1(d)$

M_T=40 N_m, M_{max}=1000 N_m, f_m=0.15, f_1=0.15, α=1.5, R_e=627 MP_a, N_m=8, N_{max}=100, R_M=50 mm, R_{max}=1000 mm, C=5 mm, $\beta_1=\beta_2=\beta_3=1$, $6\le d\le 24$, $8\le N\le 100$, $50\le R_B\le 1000$, $40\le M\le 1000$.

3. Optimization algorithm

We used ten non-traditional optimization methods to optimize the coupling with bolted rim problem.

The methods used for optimization are,

1. Particle swarm optimization (PSO), (James *et al. 2018*)
2. Crow search algorithm (CSA),
3. Enhanced honeybee mating optimization (EHBMO),
4. Harmony search algorithm (HSA),
5. Krill heard algorithm (KHA),
6. Pattern search algorithm (PSA),
7. Charged system search algorithm (CSSA),

Table 1 Comparison of the best optimum solution for the coupling with bolted rim problem

	PSO	**EHBMO**	**HSA**	**CSA**	**CSSA**	**BBCO**	**GBA**	**KHA**	**PSA**	**SSA**
d (mm)	**6.0000**	6.0031	6.2374	6.1122	6.6425	6.4565	6.5452	6.5728	6.2563	6.1346
N	**8**	8.0027	8.186348	8.2564	8.6926	8.5645	8.5555	8.5715	8.5469	8.0055
Rb (mm)	**56.5432**	59.4900	58.9047	58.2356	59.6737	58.6596	58.9493	58.6012	57.8659	57.40388
M (Nm)	**40**	40.2163	40.2588	40.9856	40.6354	40.3265	40.5616	40.6584	40.2355	40.00484
f_{min}	**3.27**	3.4854	3.4529	3.5236	3.46653	3.48569	3.4824	3.48604	3.312566	3.314609

d-diameter of the bolts (mm), *N*-number of bolts, *M*-adhesion of torque (Nm), R_B-radius (mm)

Table 2 Bound of the variables

Boundaries	*d*	*N*	$\boldsymbol{R_B}$	*M*
Upper boundary	24	100	1000	1000
Lower boundary	6	8	50	40
Optimum	6.00	8.00	56.54	40.00

8. Salp swarm algorithm (SSA),
9. Big bang big crunch optimization (B-BBBCO),
10. Gradient based Algorithm (GBA).

These methods are swarm-based, meta-heuristic, population based, intelligent based algorithms.

Table 1 shows the comparison of the best optimum solution for the coupling with bolted rim problem.

The coupling with bolted rim was designed according to the given dimensions. Cast Iron material was taken as the material of the coupling with bolted rim.

4. ANSYS simulation

ANSYS is a finite-element modelling tool that may be used to solve a wide range of mechanical problems numerically (Ackshaya *et al.* 2021). Static/dynamic, structural analysis, heat transmission, as well as fluid problems, along with acoustic and electromagnetic challenges, are among these issues. Simulation is used to examine the feasibility of reducing coupling with bolted rim design. Ansys software was used to simulate the situation (Ion). Table 2 shows the bounds of the variables.

4.1 Coupling with bolted rim

The coupling with bolted rim dimension:
FLANGE OD: 190 mm
HUB OD: 90 mm
DRIVEN & DRIVER SHAFT OD: 45 mm
DRIVEN & DRIVER SHAFT LENGTH: 120 mm
FLANGE THICKNESS: 20 mm

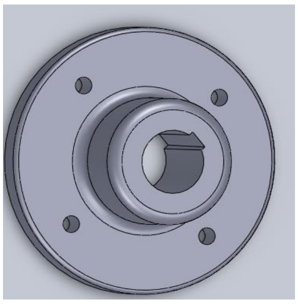

Fig. 2 Flange

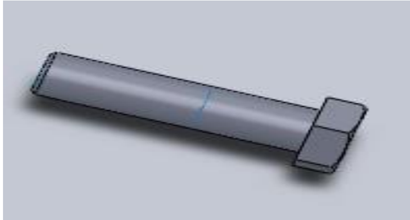

Fig. 3 Bolt

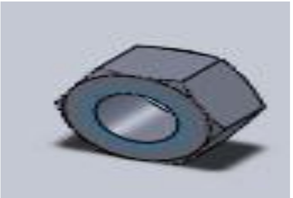

Fig. 4 Nut

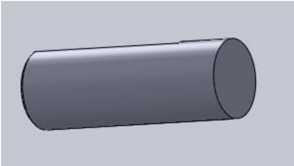

Fig. 5 Shaft

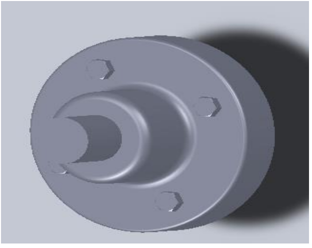

Fig. 6 Coupling with bolted rim assembly

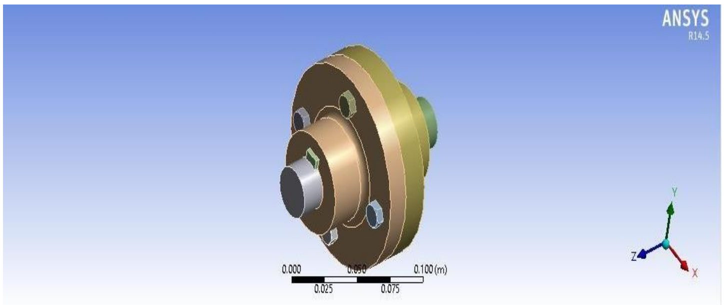

Fig. 7 Solid model of coupling with bolted rim

HEIGHT OF FLANGE TO HUB: 75 mm
DIAMETER OF BOLT & NUT: 12 mm

4.2 ANSYS model

The Ansys model of the coupling with bolted rim:

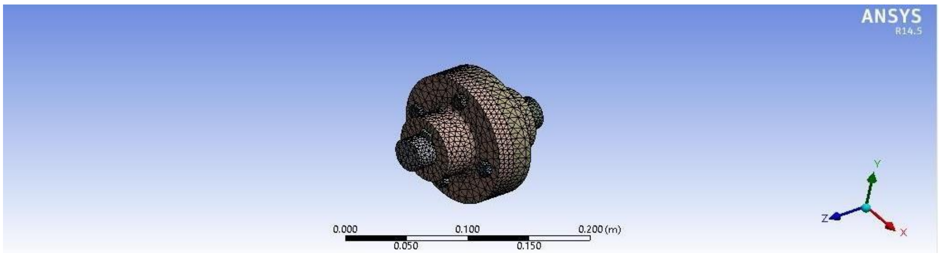

Fig. 8 Meshing of the lower boundary geometry

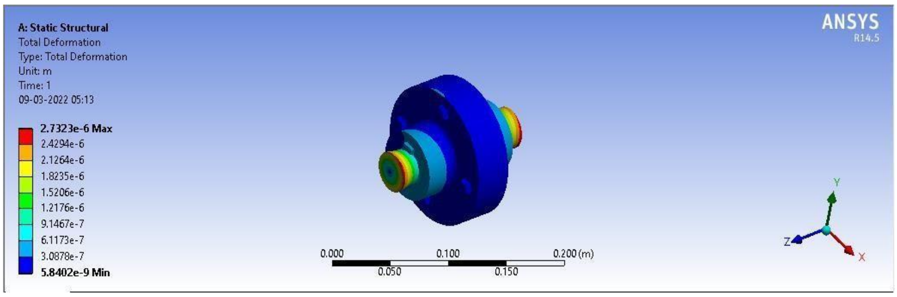

Fig. 9 Deflection

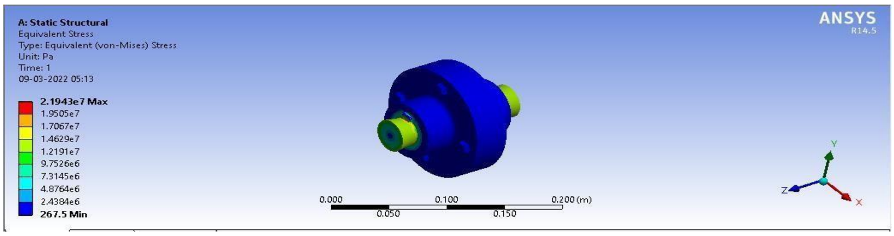

Fig. 10 Stress

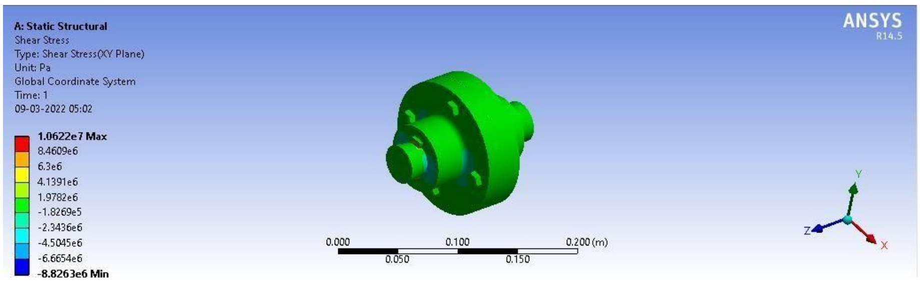

Fig. 11 Shear stress

4.3 Analysis

4.3.1 Analysis_lower

a) At Preload (40 Nm)

For the lower boundary geometry, a mesh is created (Yang *et al*. 2017) Fig. 8. Shows the mesh model for lower boundary geometry.

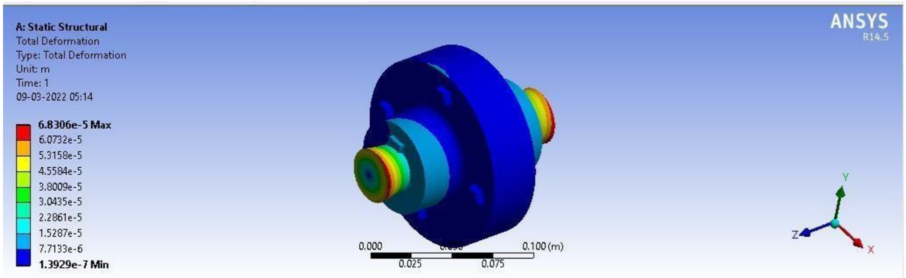

Fig. 12 Deflection

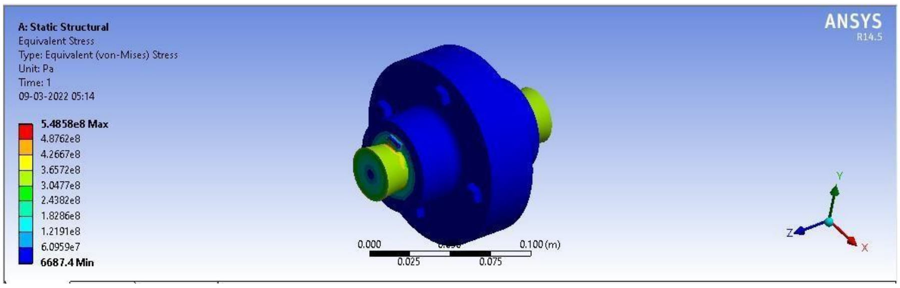

Fig. 13 Stress

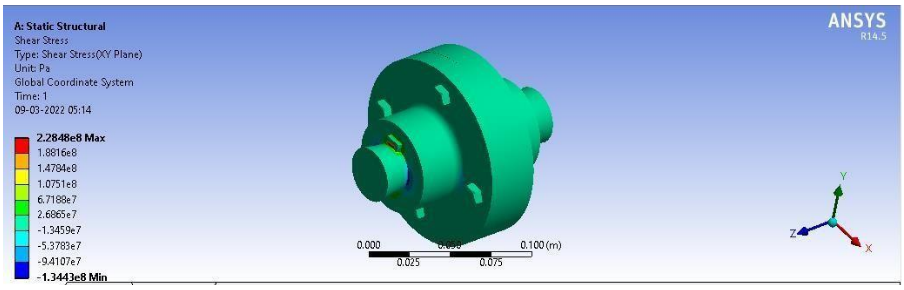

Fig. 14 Shear stress

The total deformation of the beam for lower bound geometry for preloading is given in Fig. 9. It is evident that total deformation is 2.7323e-6m.

The stress developed in the coupling with bolted rim for lower boundary geometry for preloading is seen in Fig. 10. Stress started to build up in the coupling with bolted rim is 2.1943e7 Pa.

The shear stress developed in the coupling with bolted rim for optimum boundary geometry for preloading is given in Fig. 11. Shear stress started to build up in the coupling with bolted rim is 1.0622e7 Pa.

b) At Max.load (1000 Nm)

The total deformation of the beam for lower bound geometry for max. load is given in Fig. 12. It is evident that total deformation is 6.8306e-5 m

The stress developed in the coupling with bolted rim for lower boundary geometry for max. load is seen in Fig. 13. Stress started to build up in the coupling with bolted rim is 5.4858e8 Pa.

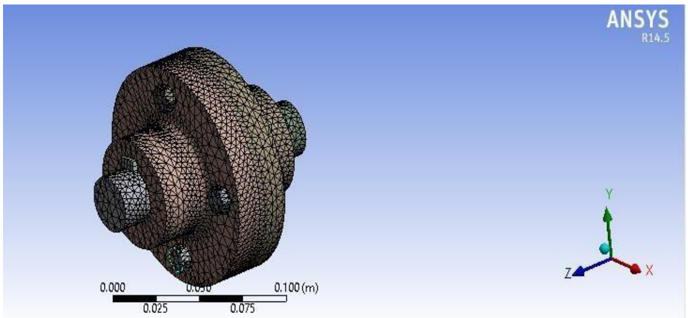

Fig. 15 Meshing of the upper boundary geometry

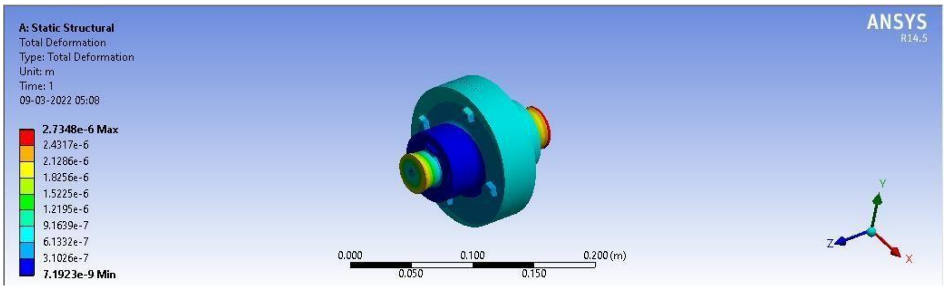

Fig. 16 Deflection

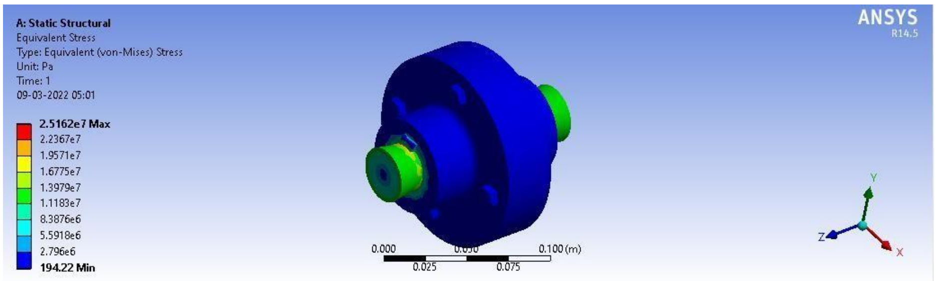

Fig. 17 Stress

The shear stress developed in the coupling with bolted rim for optimum boundary geometry for max. load is given in Fig. 14. Shear Stress started to build up in the coupling with bolted rim is 2.2848e8 Pa.

4.3.2 Analysis_upper

a) At preload (40 Nm)

The mesh for upper boundary geometry is generated, and the meshed model for upper boundary geometry is seen in Fig. 15.

The total deformation of the beam for upper boundary geometry for preloading is given in Fig. 16. It is evident that total deformation is 2.7348e-6 m.

The stress developed in the coupling with bolted rim for upper boundary geometry for preloading is seen in Fig. 17. Stress started to build up in the coupling with bolted rim is 2.5162e7 Pa.

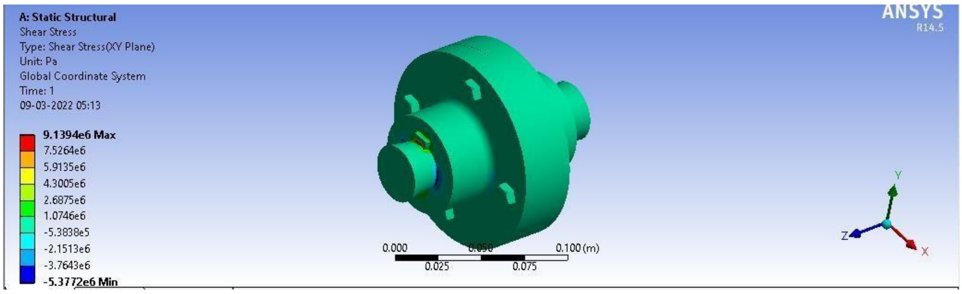

Fig. 18 Shear stress

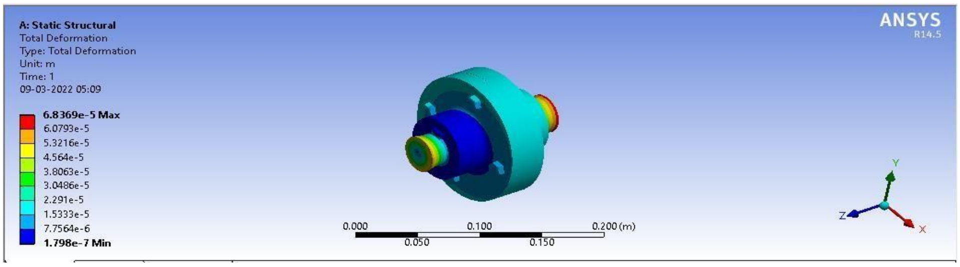

Fig. 19 Deflection

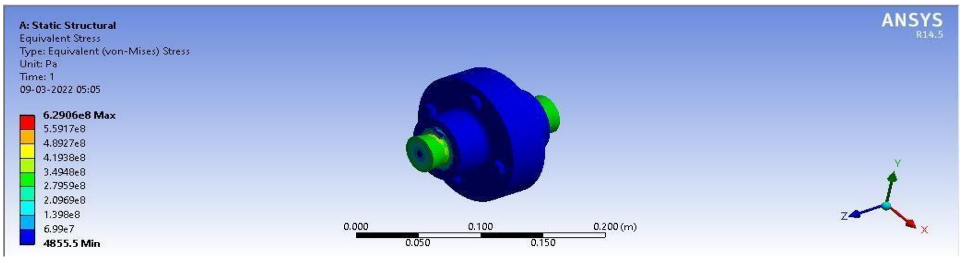

Fig. 20 Stress

The shear stress developed in the coupling with bolted rim for optimum boundary geometry for preloading is given in Fig. 18. Shear Stress started to build up in the coupling with bolted rim is 9.1394e6 Pa.

b) At Max.load (1000 Nm)

The total deformation of the beam for lower bound geometry for max. load is given in Fig. 19. It is evident that total deformation is 6.8369e-5 m

The stress developed in the coupling with bolted rim for lower boundary geometry for max. load is given in Fig. 20. Stress started to build up in the coupling with bolted rim is 6.2906e8 Pa.

The shear stress developed in the coupling with bolted rim for optimum boundary geometry for max. load is seen in Fig. 21. Shear stress started to build up in the coupling with bolted rim is 2.6555e8 Pa.

4.3.3 Analysis_optimum

a) At Preload (40 Nm)

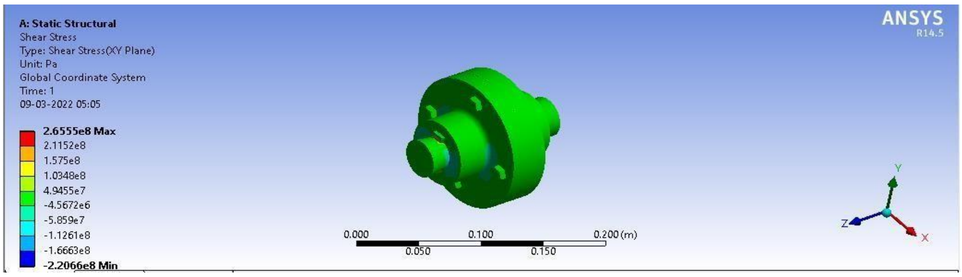

Fig. 21 Shear stress

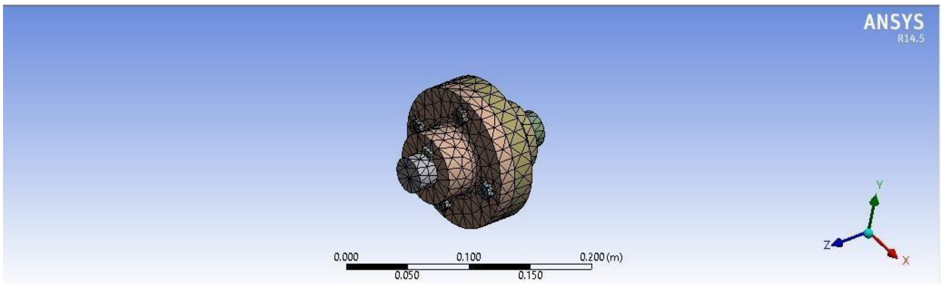

Fig. 22 Meshing of the optimum boundary geometry

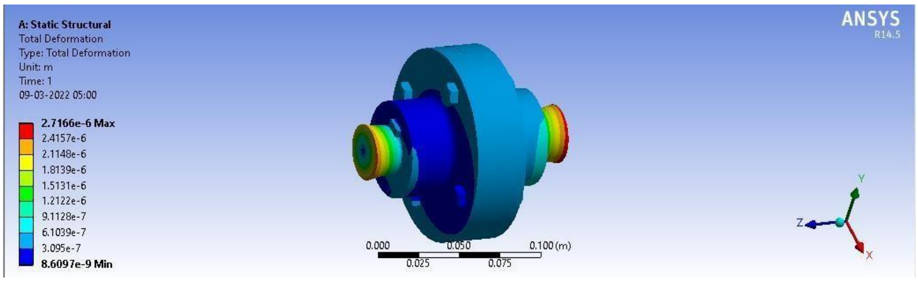

Fig. 23 Deflection

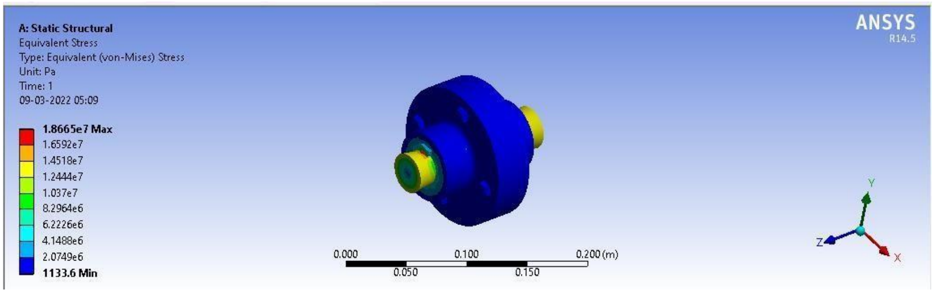

Fig. 24 Stress

The mesh is for optimum boundary geometry is generated, and the meshed model for optimum boundary geometry is seen in the Fig. 22.

The total deformation of the coupling with bolted rim for optimum boundary geometry given in Fig. 23. It is evident that total deformation is 2.7166e-6 m.

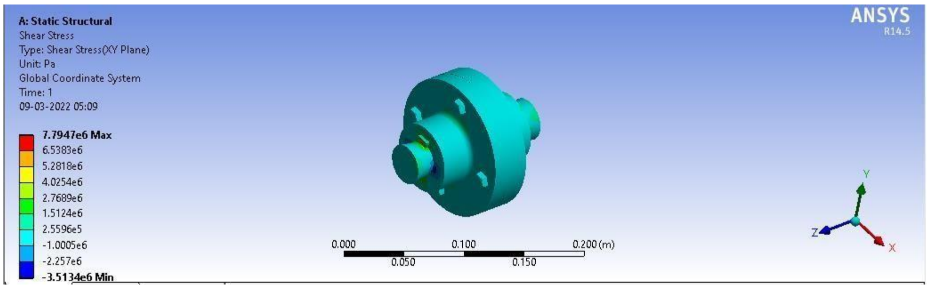

Fig. 25 Shear stress

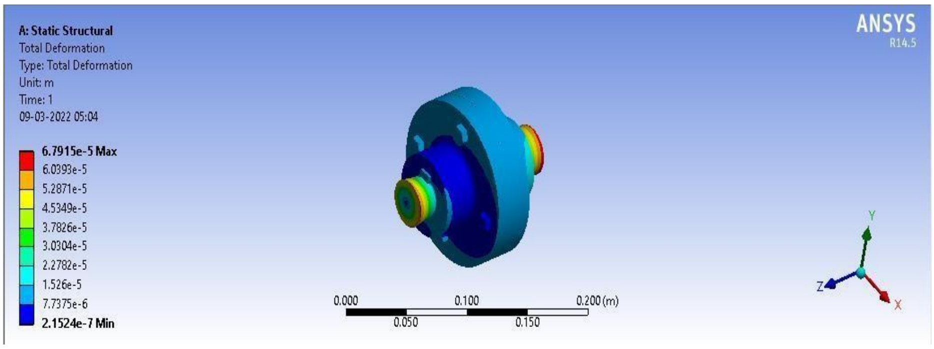

Fig. 26 Deflection

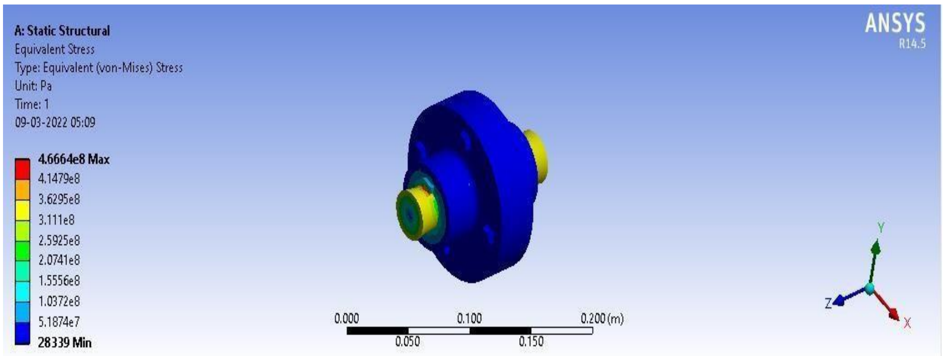

Fig. 27 Stress

The stress developed in the coupling with bolted rim for optimum boundary geometry for preloading is given in Fig. 24. Stress started to build up in the coupling with bolted rim is 1.8665e7 Pa.

The shear stress developed in the coupling with bolted rim for optimum boundary geometry for preloading is seen in Fig. 25 (Singh *et al.* 2015). Shear stress started to build up in the coupling with bolted rim is 7.7947e6 Pa.

b) At Max.load (1000 Nm)

The total deformation of the coupling with bolted rim for optimum boundary geometry given in Fig. 26. It is evident that total deformation is 6.7915e-5 m.

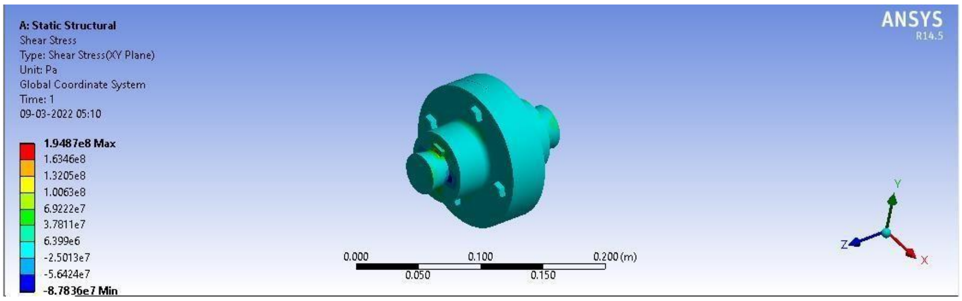

Fig. 28 Shear stress

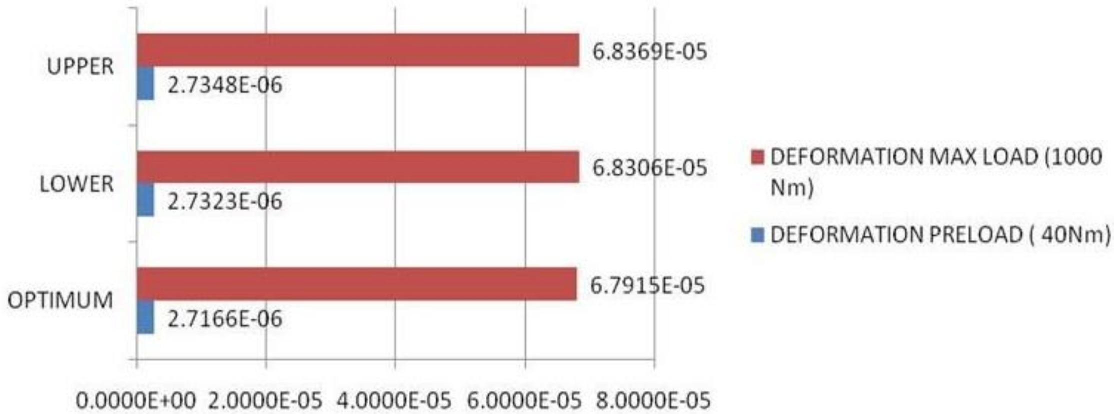

Fig. 29 Stress value

The stress developed in the coupling with bolted rim for optimum boundary geometry for max. load is given in Fig. 27. Stress started to build up in the coupling with bolted rim is 4.6664e8 Pa.

The shear stress developed in the coupling with bolted rim for optimum boundary geometry for max load is given in Fig. 28. Shear stress started to build up in the coupling with bolted rim is 1.9487e8 Pa.

5. Conclusion for simulation

In the case of optimum boundary geometry of the coupling with bolted rim, the maximum stress value is less than upper & lower boundary geometry of coupling with bolted rim which is shown in the Fig. 29.

In the case of optimum boundary geometry of the coupling with bolted rim, the maximum shear stress value is less than upper & lower boundary geometry of coupling with bolted rim which is shown in the Fig. 30 (Muftah 2021).

In the case of optimum boundary geometry of the coupling with bolted rim, the maximum Deformation value is less than upper & lower boundary geometry of coupling with bolted rim which is shown in the Fig. 31.

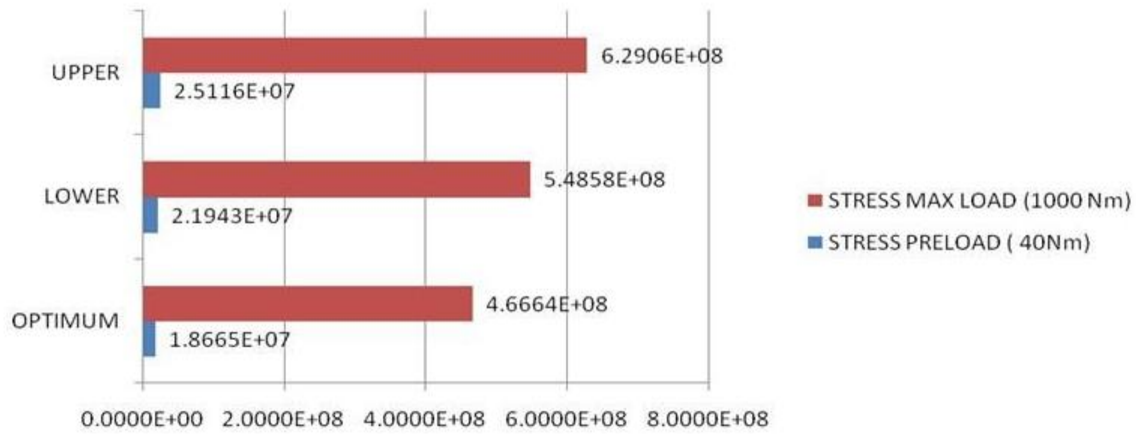

Fig. 30 Shear stress value

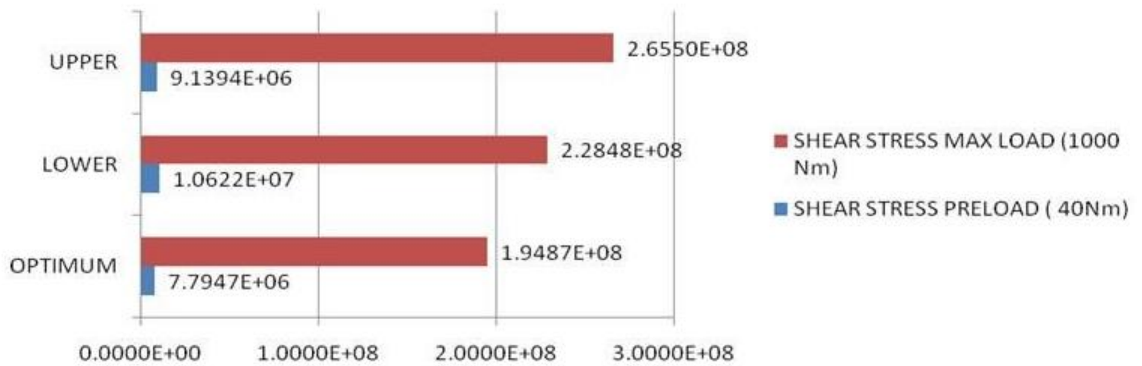

Fig. 31 Deformation value

6. Conclusions

To minimize the weight of the coupling with bolted rim, we optimized the variables, which are, the number of bolts (N), diameter of the bolts (d), adhesion of torque (M) and the radius (R_B) using ten non- traditional optimization methods. Particle Swarm Optimization (PSO) yield the minimum weight comparing to other methods. And the results are validated by ANSYS simulation. It was found that the optimum value obtained by PSO is the best optimum value.

References

Abderazek, H., Yildiz, A.R. and Sait, S.M. (2019), "Mechanical engineering design optimisation using novel adaptive differential evolution algorithm", *Int. J. Vehic. Des.*, **80**(2-4), 285-329. https://doi.org/10.1504/IJVD.2019.109873.

Elbeltagi, E., Hegazy, T. and Grierson, D. (2005), "Comparison among five evolutionary-based optimization algorithms", *Adv. Eng. Inform.*, **19**(1), 43-53. https://doi.org/10.1016/j.aei.2005.01.004.

Giraud-Moreau, L. and Lafon, P. (2002), "A comparison of evolutionary algorithms for mechanical design components", *Eng. Optim.*, **34**(3), 307-322. https://doi.org/10.1080/03052150211750.

Hilal, M.M. (2021), "Design and simulation of a piezoresistive V-shaped strain gauge for torque measring", *Scientif. J. Facult. Sci.-Sirte Univ.*, **1**(2), 41-51. https://doi.org/10.37375/sjfssu.v1i2.70.

Ion, I.O.N. Design Optimization of a Gear Speed Reducer by Way of MATLAB & Ansys.

Kennedy, J. and Eberhart, R. (1995), "Particle swarm optimization", *Proceedings of ICNN'95-International Conference on Neural Networks*, **4**, 1942-1948. https://doi.org/10.1109/ICNN.1995.488968.

Lafon, P. (1994), "Conception optimale de systèmes mécaniques: Optimisation en variables mixtes", Doctoral Dissertation, Institut National des Sciences Appliquées de Toulouse.

Singh, L., Rawat, S.S., Hasan, T. and Kumar, U. (2015), "Finite element analysis of piston in ANSYS", *Int. J. Mod. Trend. Eng. Res.*, **4**, 619-626.

Varshini, K.A., Rajan, H. and Sankararaman, R. (2021), "Numerical simulation on the effects of Ambient velocity and Temperature on solar panel efficiency", *IOP Conf. Ser.: Earth Environ. Sci.*, **850**(1), 012030. https://doi.org/10.1088/1755-1315/850/1/012030.

Yang, Z., Li, J.Y., Zhang, Y.P., Li, H.L. and Gao, X.H. (2017), "Analysis of the properties of mechanical materials and parts based on ANSYS software", *Key Eng. Mater.*, **723**, 388-393. https://doi.org/10.4028/www.scientific.net/KEM.723.388.

Yildiz, A.R., Abderazek, H. and Mirjalili, S. (2020), "A comparative study of recent non-traditional methods for mechanical design optimization", *Arch. Comput. Meth. Eng.*, **27**(4), 1031-1048. https://doi.org/10.1007/s11831-019-09343-x12.